

# Averaged dynamics of soliton molecules in dispersion-managed optical fibers

S. M. Alamoudi<sup>1</sup>, U. Al Khawaja<sup>2</sup>, and B. B. Baizakov<sup>3</sup>

<sup>1</sup> *Department of Physics, King Fahd University of Petroleum and Minerals, Dhahran 31261, Saudi Arabia*

<sup>2</sup> *Physics Department, United Arab Emirates University, P.O. Box 15551, Al-Ain, United Arab Emirates*

<sup>3</sup> *Physical-Technical Institute, Uzbek Academy of Sciences, 100084, Tashkent, Uzbekistan*

(Dated: March 27, 2018)

The existence regimes and dynamics of soliton molecules in dispersion-managed (DM) optical fibers have been studied. Initially we develop a variational approximation (VA) for description of periodic dynamics of a soliton molecule within each unit cell of the dispersion map. The obtained system of coupled equations for the pulse width and chirp allows to find the parameters of DM soliton molecules for the given dispersion map and pulse energy. Then by means of a scaling transformation and averaging procedure we reduce the original nonlinear Schrödinger equation (NLSE) with piecewise-constant periodic dispersion to its counterpart with constant coefficients and additional parabolic potential. The obtained averaged NLSE with expulsive potential can explain the essential features of solitons and soliton molecules in DM fibers related to their energy loss during propagation. Also, the model of averaged NLSE predicts the instability of the temporal position of the soliton, which may lead to difficulty in holding the pulse in the middle of its time slot. All numerical simulations are performed using the parameters of the existing DM fiber setup, and illustrated via pertinent examples.

## I. INTRODUCTION

During the last two decades the amount of information transmitted via optical fiber communication systems has increased enormously. High performance of modern communication lines is provided by an optical fiber [1], where the information is encoded and transmitted as a sequence of light pulses. Despite the very high data rate achieved today ( $\sim 50$  TB/s over single fiber), there is urgent demand for even more capacity of the fiber line, originating from the needs of telecommunications and the Internet. Different approaches are being pursued to address the capacity problem, such as improving the transmission properties of the optical fiber, lying additional parallel cables and using the information coding schemes going beyond the binary format, which is currently employed. Among the above mentioned approaches using the extended alphabet, where a bound state of two or more optical solitons called *soliton molecule* serves as a new carrier of information unit [2], seems to be most appealing because it employs already existing optical fiber lines, and therefore is beyond the competition from the viewpoint of cost-effectiveness.

It is appropriate to recall that solitons are self-localized wave packets that can propagate along wave-guides preserving their shape and velocity, and exhibit particle-like collisions with each-other. Bright solitons emerge from the fine balance between the dispersive broadening and nonlinear self-focusing of the wave packet. When the optical soliton was theoretically predicted [3] and experimentally observed [4], there was a promising idea that it can be used as information carrier in optical fiber communication systems [5] due to its exceptional robustness against perturbations. Besides, the nonlinearity of the optical fiber, considered to be nuisance in linear systems, has been used as an advantage in this case as it provides the soliton's self-healing property. However, some other detrimental effects like four-wave mixing and Gordon-Haus timing jitter [6] have imposed difficulties for the progress in this direction. Later the concept of dispersion-management (DM) and DM soliton was put forward (for a recent review see [7]), which allowed to suppress these adverse effects, and eventually has led to realization of several commercial soliton based optical fiber communication systems. An interesting chronicle of the growth of the telecommunications industry, including the fiber optic systems, is given in Ref. [1].

Recent progress in using solitons for information transfer is linked to the observation, that solitons in DM fibers can form stable bound states called soliton molecules, and realizing their potential for enhancing the capacity of the communication system via extension of the coding alphabet [2]. The binding mechanism of solitons in the molecule was proposed in [8]. The proof-of-principle demonstration of the data transmission via optical fiber using the extended alphabet: logical *zero*, *one* (single soliton), *two* (two-soliton molecule) and *three* (three-soliton molecule), was recently reported in [9, 10]. The practical implementation of this novel approach requires extensive research on the existence regimes, stability, mutual interactions and propagation dynamics of soliton molecules in DM fibers.

In this work we study the existence regimes and dynamics of soliton molecules in DM fibers by analytical and numerical means. First we develop a variational approach (VA) to find the stationary shape of the molecule and equilibrium separation between solitons in the molecule. At this stage we obtain two coupled ordinary differential equations (ODE) for the temporal separation between solitons and chirp parameter, which describes the fast dynamics of the molecule within a unit cell of the DM fiber. Although the derived ODE system is capable of describing the propagation of the molecule for arbitrary distance, long-haul transmission of DM solitons and molecules is conve-

nient to explore using the averaged nonlinear Schrödinger equation (NLSE). The averaged NLSE can help to specify the existence regimes of solitons and molecules, elucidate the physical mechanism by which they lose energy, and eventually disintegrate in conservative DM fibers.

The paper is organized as follows. In the next Sec. II we introduce the NLSE which governs the pulse propagation in DM fibers. Here we also present the parameters of the DM fiber used in our calculations. In Sec. III we develop the VA for the fast dynamics of solitons and molecules and compare its predictions with the results of PDE simulations. Then we derive in Sec. IV the averaged NLSE and determine its coefficients using the VA. Here we also perform the analysis of the pulse propagation in the NLSE with inverted parabolic potential. In Sec. V we summarize our findings.

## II. THE GOVERNING EQUATION

Propagation of optical pulses in fibers with inhomogeneous parameters is described by the following nonlinear Schrödinger equation

$$i \frac{\partial E}{\partial z} - \frac{\beta(z)}{2} \frac{\partial^2 E}{\partial t^2} + \Gamma(z)|E|^2 E = ig(z)E, \quad (1)$$

where  $E(z, t)$  ( $|E|^2$  [ $W$ ]),  $z$  [ $m$ ], and  $t$  [ $s$ ] are respectively, the complex envelope of the electric field, the propagation distance, and the retarded time. The coefficients  $\beta(z)$  [ $s^2/m$ ],  $\Gamma(z)$  [ $1/(W \cdot m)$ ], and  $g(z)$  [ $1/m$ ] represent the fiber's group velocity dispersion (GVD), nonlinearity and gain/loss parameter, respectively. Here and below in rectangular brackets  $[\cdot \cdot \cdot]$  we show the physical unit of the corresponding variable.

For qualitative analysis and numerical simulations it is convenient to reduce the Eq. (1) into dimensionless form. At first we eliminate the gain/loss term via new variable  $u(z, t)$  ( $|u|^2$  [ $W$ ]), following Ref. [11]

$$E(z, t) = a(z)u(z, t), \quad a(z) = a_0 \exp \left[ \int_0^z g(\xi) d\xi \right], \quad (2)$$

where  $a_0$  is dimensionless constant. The new complex function  $u(z, t)$  satisfies the equation

$$i \frac{\partial u}{\partial z} - \frac{\beta(z)}{2} \frac{\partial^2 u}{\partial t^2} + \gamma(z)|u|^2 u = 0, \quad (3)$$

where  $\gamma(z) = a^2(z) \cdot \Gamma(z)$  is the fiber's effective nonlinearity. Now we convert the Eq. (3) into standard form with constant nonlinearity by introducing the new coordinate  $z'$  [ $1/W$ ] defined by  $z'(z) = \int_0^z \gamma(\xi) d\xi$

$$i \frac{\partial u}{\partial z'} - \frac{\beta'(z')}{2} \frac{\partial^2 u}{\partial t^2} + |u|^2 u = 0, \quad (4)$$

where  $\beta'(z') = \beta(z')/\gamma(z')$  [ $W \cdot s^2$ ] is the fiber's effective dispersion, characterizing both the fiber's GVD and nonlinearity. The original parameters  $\beta(z)$ ,  $\Gamma(z)$  and  $g(z)$  in Eq. (1) are periodic functions of propagation distance with common period  $L$ , while the effective dispersion  $\beta'(z')$  in Eq. (4) is a periodic function with period defined by

$$L' = \int_0^L \gamma(\xi) d\xi = L^+ \gamma^+ + L^- \gamma^-, \quad [1/W]. \quad (5)$$

To obtain the final equation we introduce dimensionless variables

$$q(Z, T) = u(z', t) \cdot \sqrt{L'}, \quad Z = z'/L' \quad T = t/\tau_m, \quad (6)$$

where  $\tau_m$  is the characteristic time scale equal to pulse duration of the laser source  $\tau_{fwhm}$ . In terms of these variables the dimensionless governing equation acquires the form

$$i \frac{\partial q}{\partial Z} - \frac{D(Z)}{2} \frac{\partial^2 q}{\partial T^2} + |q|^2 q = 0, \quad (7)$$

where  $D(Z) = \beta'(Z)L'/\tau_m^2$  represents the fiber's dimensionless effective dispersion. To show the results in dimensional variables we solve the equation

$$\int_0^z \gamma(\xi) d\xi = Z \cdot L', \quad (8)$$

with respect to  $z$  [m], for given dimensionless propagation distance  $Z$ , the period  $L'$  [1/W], and known nonlinear map function  $\gamma(z)$  [1/(W · m)]. The original time  $t$  [s] and field amplitude  $u$  [ $\sqrt{W}$ ] are restored via Eq.(6). Note that  $z = L$  corresponds to  $Z = 1$ , in accordance with Eq. (5).

In the absence of gain/loss term in Eq. (1), i.e.  $g(z) = 0$

$$a(z) \equiv a_0, \quad a_0 = \left( \frac{L}{\int_0^L \exp[2 \cdot \int_0^z g(\xi) d\xi] dz} \right)^{1/2} = 1. \quad (9)$$

The dimensionless pulse energy is

$$E_0 = \int_{-\infty}^{\infty} |q|^2 dT = \frac{L'}{\tau_m} \cdot \int_{-\infty}^{\infty} |u|^2 dt = \frac{L'}{\tau_m} \cdot \mathcal{E}_0, \quad (10)$$

where  $\mathcal{E}_0$  [J] - is the original pulse energy.

### A. Parameters of the dispersion map

In the following sections we employ the DM map parameters, corresponding to the setup of Ref. [9, 10], for laser wavelength  $\lambda = 1540$  nm

$$\beta_2^+ = + 4.259 \text{ [ ps}^2/\text{km ]}, \quad \gamma^+ = 1.7 \text{ [ 1/(W} \cdot \text{km) ]}, \quad L^+ = 22 \text{ [ m ] (positive GVD fiber),}$$

$$\beta_2^- = - 5.159 \text{ [ ps}^2/\text{km ]}, \quad \gamma^- = 1.7 \text{ [ 1/(W} \cdot \text{km) ]}, \quad L^- = 24 \text{ [ m ] (negative GVD fiber).}$$

The period of the original DM map is  $L = L^+ + L^- = 46$  [ m ]. For the effective dispersion in Eq. (4) the period is  $L' = \gamma^+ \cdot L^+ + \gamma^- \cdot L^- = 0.078$  [ 1/W ]. The path averaged dispersion and nonlinearity are equal to

$$\bar{\beta}_2 = (\beta_2^+ \cdot L^+ + \beta_2^- \cdot L^-) / L = - 0.655 \text{ [ ps}^2/\text{km ]}, \quad \bar{\gamma} = (\gamma^+ \cdot L^+ + \gamma^- \cdot L^-) / L = 1.7 \text{ [ 1/(W} \cdot \text{km) ]}.$$

The characteristic time, length and energy scales are given below

$$\tau_{fwhm} = 0.25 \text{ [ ps ]}, \quad T_0 = \tau_{fwhm} / 1.67 = 0.15 \text{ [ ps ] (pulse duration),}$$

$$L_D = T_0^2 / |\bar{\beta}_2| = 0.034 \text{ [ km ] (dispersion length),}$$

$$S = (|\beta_2^+ - \bar{\beta}_2| \cdot L^+ + |\beta_2^- - \bar{\beta}_2| \cdot L^-) / \tau_{fwhm}^2 = 3.459 \text{ (strength of the map).}$$

From the above presented data we get the dimensionless map parameters

$$D_1 = (\beta_2^- / \gamma^-) \cdot (L' / \tau_{fwhm}^2) = - 3.796, \quad L_1 = L^- \cdot \gamma^- / L' = 0.522,$$

$$D_2 = (\beta_2^+ / \gamma^+) \cdot (L' / \tau_{fwhm}^2) = + 3.135, \quad L_2 = L^+ \cdot \gamma^+ / L' = 0.478,$$

$$\Delta D = (D_1 \cdot L_1 + D_2 \cdot L_2) / (L_1 + L_2) = - 0.482, \quad L_1 + L_2 = 1.$$

Figure 1 shows the dispersion profiles for the original and reduced governing equations.

## III. THE VARIATIONAL APPROACH FOR FAST DYNAMICS OF SOLITON MOLECULES

Propagation of a DM soliton is characterized by fast variation of the pulse shape within each period of the DM map and slow variations on longer distances when observed stroboscopically, i.e. once per dispersion period. The periodic dynamics is compromised by different imperfections of the fiber, continuous emission of linear waves by the soliton and non-perfect initial shape of the DM soliton injected into the fiber. To compensate for the power loss and other distortions, in practice the pulses are regenerated by amplifiers which are equidistantly installed along the fiber line.

The variational approach, initially developed for description of optical soliton propagation in homogeneous fibers [12], later was successfully applied to DM solitons [13] and antisymmetric solitons in DM fibers [14, 15]. The advantages and disadvantages of the VA as compared to other methods of exploring DM solitons are discussed in [16, 17]. Below we elaborate the VA for two- and three-soliton molecules in DM fibers, based on the reduced NLSE (7).

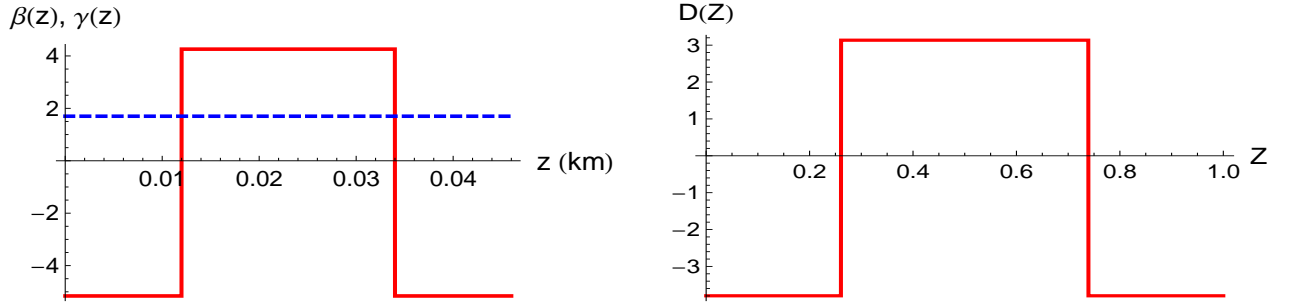


FIG. 1: Dispersion profile for one period of the DM map. Red solid line represents the piecewise-constant dispersion, blue dashed line is the parameter of nonlinearity. Left panel: For the original Eq. (3). Right panel: For reduced dimensionless Eq. (7). Note that here the coefficient of nonlinearity is equal to one and has not been shown in Eq. (7) and figure.

The Eq. (7) can be obtained from the following Lagrangian density (for tidier notations we again use small letters instead of capitals)

$$\mathcal{L} = \frac{i}{2} (qq_z^* - q^*q_z) - \frac{d(z)}{2} |q_t|^2 - \frac{1}{2} |q|^4. \quad (11)$$

To derive the VA equations we consider the shape of the soliton molecule in general form [13, 18]

$$q(z, t) = \frac{1}{\tau^{1/2}} \cdot f(t/\tau) \cdot e^{i\alpha t^2 + i\sigma}, \quad (12)$$

where  $\alpha(z), \sigma(z)$  are the chirp parameter and phase,  $\tau(z)$  is the pulse duration (proportional to the separation between solitons in the molecule),  $f(x)$  is the real function which represents the stationary shape of the soliton molecule. The energy of the pulse is (subscript zero in Eq. (10) is dropped)

$$E = \int_{-\infty}^{\infty} |q|^2 dt = \int_{-\infty}^{\infty} f^2(x) dx, \quad x = t/\tau. \quad (13)$$

Substitution of the trial function (12) into Eq. (33) yields the Lagrangian density

$$\mathcal{L} = \tau \alpha_z x^2 f^2 + \frac{\sigma_z}{\tau} f^2 - \frac{1}{2} \frac{d(z)}{\tau^3} f_x^2 - 2d(z) \tau \alpha^2 x^2 f^2 - \frac{1}{2\tau^2} f^4. \quad (14)$$

The averaged Lagrangian is obtained by integrating the last expression over the reduced time variable

$$L = \alpha_z \tau^2 \int_{-\infty}^{\infty} x^2 f^2 dx + \sigma_z \int_{-\infty}^{\infty} f^2 dx - \frac{d(z)}{2\tau^2} \int_{-\infty}^{\infty} f_x^2 dx - 2d(z) \alpha^2 \tau^2 \int_{-\infty}^{\infty} x^2 f^2 dx - \frac{1}{2\tau} \int_{-\infty}^{\infty} f^4 dx, \quad (15)$$

with a few integral constants, determined solely by the pulse shape  $f(x)$ . The Euler-Lagrange equations with respect to variational parameters  $\tau, \alpha, \sigma$  give rise to a coupled set of ODE's

$$\tau_z = -2d(z) \alpha \tau, \quad (16)$$

$$\alpha_z = -2d(z) \left( \frac{c_1}{4\tau^4} - \alpha^2 \right) - \frac{c_2}{4\tau^3}, \quad (17)$$

where

$$c_1 = \int_{-\infty}^{\infty} f_x^2 dx / \int_{-\infty}^{\infty} x^2 f^2 dx, \quad c_2 = \int_{-\infty}^{\infty} f^4 dx / \int_{-\infty}^{\infty} x^2 f^2 dx. \quad (18)$$

We adopt the following trial functions  $f(x)$  to specify the shapes of the pulses and define the corresponding parameters

$$\text{single soliton : } f(x) = A e^{-x^2}, \quad E = A^2 \cdot \sqrt{\frac{\pi}{2}}, \quad c_1 = 4, \quad c_2 = \frac{4 \cdot E}{\sqrt{\pi}}. \quad (19)$$

$$\text{2-soliton molecule : } f(x) = A x e^{-x^2}, \quad E = \frac{A^2}{4} \cdot \sqrt{\frac{\pi}{2}}, \quad c_1 = 4, \quad c_2 = \frac{E}{\sqrt{\pi}}. \quad (20)$$

$$\text{3-soliton molecule : } f(x) = A(4x^2 - 1) e^{-x^2}, \quad E = A^2 \sqrt{2\pi}, \quad c_1 = 4, \quad c_2 = \frac{41 E}{80 \sqrt{\pi}}. \quad (21)$$

The fixed point  $(\tau_0, \alpha_0)$  of the coupled system (16)-(17), which can be found using the Nijhof's method for VA models [19], defines the stationary shapes of the pulses with given energy  $E$  and DM map function  $d(z)$ . In Fig. 2 we illustrate the shapes of the two-soliton and three-soliton molecules, which are found by solving the VA system (16)-(17) and compare with the corresponding results of the Nijhof's method applied to the original Eq. (7). In Fig. 3 we show

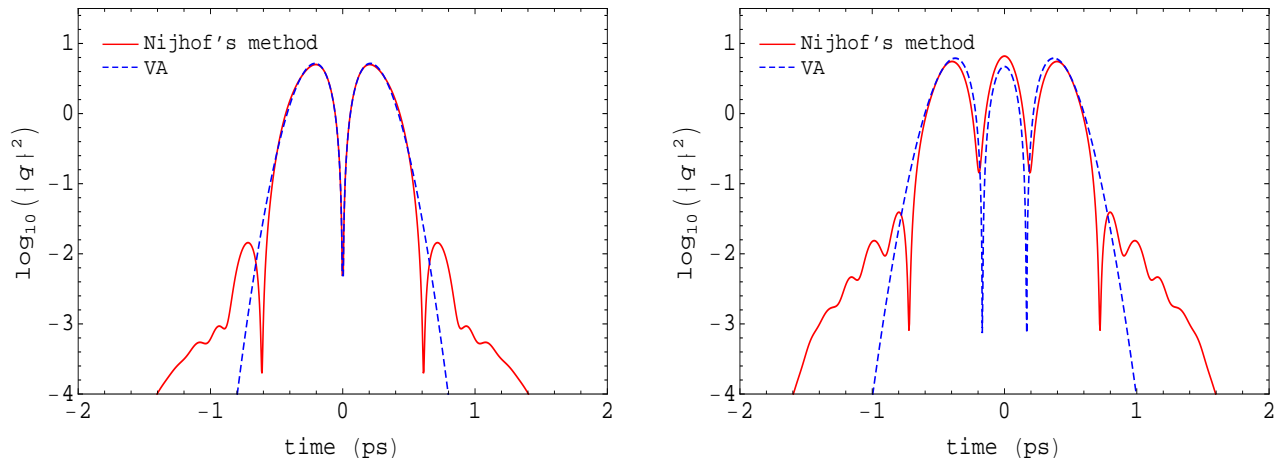


FIG. 2: Pulse shapes of the two-soliton molecule (left panel) and three-soliton molecule (right panel) in logarithmic scale. Red solid lines correspond to waveforms found by Nijhof's method [19] applied to original NLSE (7), while blue dashed lines are the prediction of VA equations (16)-(17). Appreciable deviations of the two waveforms are seen only in far tails, where the pulse amplitude is less than a percent of the maximum value. The parameters for the 2-soliton molecule:  $E_0 = 10.448$  (in original units  $\mathcal{E}_0 = 20$  pJ),  $\tau_0 = 1.1828$ ,  $A_0 = \frac{2}{\tau_0} \sqrt{\frac{E_0}{\tau_0}} \sqrt{2/\pi} = 4.489$ . For the 3-soliton molecule:  $E_0 = 15.672$  ( $\mathcal{E}_0 = 30$  pJ),  $\tau_0 = 1.333$ ,  $A_0 = \sqrt{\frac{E_0}{\tau_0 \sqrt{2\pi}}} = 2.166$ .

the phase trajectory for the periodic solution of the VA system (16)-(17) and temporal center-of-mass positions of solitons in the two-soliton molecule while it propagates along the fiber. The center-of-mass position of the right/left soliton is calculated from the solution of the VA system (16)-(17) as  $\tau_{cm}(z) = \pm\tau(z)\sqrt{2/\pi}$ , while for the NLSE (7) the corresponding formula is

$$\tau_{cm}(z) = \pm \frac{2}{E_0} \int_0^\infty t |q(z, t)|^2 dt, \quad (22)$$

where in actual calculations we use the temporal domain's half length as the upper limit of the integration. For evaluation of the pulse width and chirp parameter from the solution of Eq. (7) we employ the following expressions [19].

$$\tau(z) = \left( \frac{4}{3E} \int_{-\infty}^\infty t^2 \cdot |q(z, t)|^2 dt \right)^{1/2}, \quad \alpha(z) = \frac{\int_{-\infty}^\infty \text{Im}(q^2(z, t) \cdot q_t^*(z, t)) dt}{\int_{-\infty}^\infty |q(z, t)|^4 dt}. \quad (23)$$

As can be seen from Fig. 3 the dynamics of the pulse width is described by the VA equations quite accurately, while for the chirp parameter the agreement is only qualitative. It should be noted that although the chirp parameter shows complicated behavior within the map period, "zero chirp" condition in the middle of each anomalous GVD fiber is well satisfied.

#### IV. AVERAGED EQUATION FOR SOLITON MOLECULES IN DM FIBERS

Long-haul propagation of soliton molecules in DM fibers is convenient to study using the averaged NLSE. The averaging procedure was developed in [13, 18]. Below we use the approach based on the scaling arguments proposed in Ref. [20] and look for the solution of Eq. (7) in the form (capital letters changed to lower-case)

$$q(z, t) = w(z, t) e^{i\alpha(z)t^2}, \quad (24)$$

where  $\alpha(z)$  is the chirp parameter. Inserting this into the governing Eq. (7) we obtain

$$i(w_z - 2d\alpha t w_t) - \frac{d}{2} w_{tt} + (2d\alpha^2 - \alpha_z) t^2 w + |w|^2 w = id\alpha w. \quad (25)$$

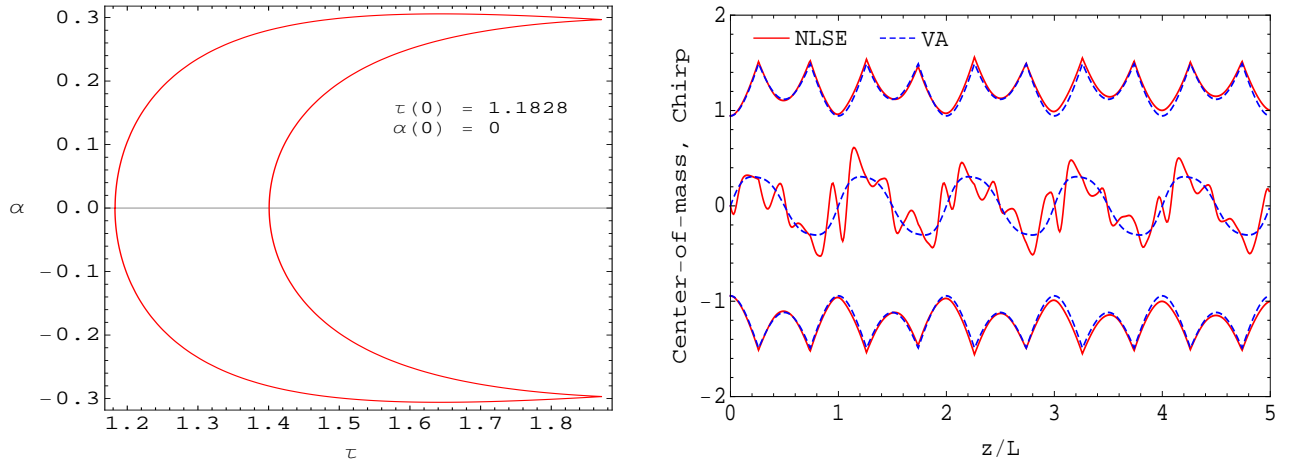


FIG. 3: Left panel: Closed phase trajectory indicates that the fixed point  $\tau(0) = 1.1828$ ,  $\alpha(0) = 0$  corresponds to the periodic solution of the system (16)-(17) for a two-soliton molecule with energy  $E = 10.448$ , shown in Fig.2. Right panel: The solution of the NLSE (7) with the initial pulse shape predicted by the VA shows that solitons in the two-soliton molecule perform oscillatory motion periodically reducing and increasing the temporal separation between their center-of-mass positions (top and bottom curves). The evolution of the chirp parameter (middle curve) shows qualitative agreement with the VA.

By introducing the new time ( $x$ ) and amplitude ( $b$ ) functions

$$x = t/\tau(z), \quad w(z, t) = b(z) v(z, x). \quad (26)$$

the last equation can be reduced into the form

$$i \left( b v_z + b_z v - \frac{b t \tau_z}{\tau^2} v_x - \frac{2 b d \alpha t}{\tau} v_x \right) - \frac{b d}{2 \tau^2} v_{xx} - (\alpha_z - 2 d \alpha^2) t^2 b v + b^3 |v|^2 v = i d \alpha b v. \quad (27)$$

When the following relations are satisfied

$$b_z = d \alpha b, \quad \tau_z = -2 d \alpha \tau, \quad (28)$$

the NLSE with a parabolic potential results from Eq. (27)

$$i v_z - \frac{d}{2 \tau^2} v_{xx} + b^2 |v|^2 v - (\alpha_z - 2 d \alpha^2) \tau^2 x^2 v = 0. \quad (29)$$

The amplitude function is linked to the pulse width as  $b(z) = \beta/\sqrt{\tau(z)}$ , which can be readily verified from Eq. (28). The constant  $\beta$  is specified by the selected trial function. Now applying the averaging procedure to Eq. (29) we obtain in leading order

$$i \psi_z + d_0 \psi_{xx} + b_0 |\psi|^2 \psi + k_0 x^2 \psi = 0, \quad (30)$$

where  $\psi(z, x)$  is the slowly varying core of the DM soliton. The quantities averaged over one dispersion period are defined as  $d_0 = -\frac{1}{2} \langle d(z)/\tau^2(z) \rangle$ ,  $b_0 = \beta^2 \langle 1/\tau(z) \rangle$ ,  $k_0 = \langle [2d(z)\alpha^2(z) - \alpha_z(z)] \tau^2(z) \rangle$ . The averaging is performed as  $\langle \phi(z) \rangle = \int_0^1 \phi(z) \tau(z) dz / \int_0^1 \tau(z) dz$  (for the reduced map period  $L = 1$ ). In numerical implementation of the averaging procedure we employ the periodic solution of VA Eqs. (16)-(17). In particular from Eq. (17) it follows that  $k_0 = (c_1/2) \langle d(z)/\tau^2(z) \rangle + (c_2/4) \langle 1/\tau(z) \rangle$ , with constants  $c_1, c_2$  given by Eq. (18). For the DM map parameters specified in Sec. IIA all coefficients of Eq. (30) appear to be positive ( $d_0 > 0$ ,  $b_0 > 0$ ,  $k_0 > 0$ ), therefore we have gotten the NLSE with anomalous dispersion, focusing nonlinearity and inverted parabolic potential. This equation is formally similar to the quantum mechanical equation for a wave packet, evolving under the effective potential

$$U(z, x) = -b_0 |\psi(z, x)|^2 - k_0 x^2. \quad (31)$$

The stationary solution  $\psi(z, x) = \varphi(x) e^{i\lambda z}$  can be found from the initial value problem with respect to variable  $x$

$$d_0 \varphi_{xx} + b_0 \varphi^3 + k_0 x^2 \varphi - \lambda \varphi = 0, \quad (32)$$

and suitable initial conditions  $\varphi(0)$  and  $\varphi_x(0)$ .

It is appropriate to mention that Eq. (30) with additional gain/loss term was previously considered also in other contexts, such as the nonlinear compression of chirped optical solitary waves [23], and with regard to integrability issues [24–27].

### A. The variational approach for averaged NLSE

To study the evolution of pulses governed by Eq. (30) we develop the VA. The corresponding Lagrangian density is

$$\mathcal{L} = \frac{i}{2}(\psi\psi_z^* - \psi^*\psi_z) + d_0|\psi_x|^2 - k_0x^2|\psi|^2 - \frac{b_0}{2}|\psi|^4. \quad (33)$$

The trial function will be of the form

$$\psi(x, t) = A\eta(x) e^{-(x-\xi)^2/\tau^2 + i\alpha(x-\xi)^2 + iv(x-\xi) + i\varphi}, \quad (34)$$

where  $A(z)$ ,  $\tau(z)$ ,  $\xi(z)$ ,  $v(z)$ ,  $\alpha(z)$ ,  $\varphi(z)$  are variational parameters, designating the pulse amplitude, width, center of mass position, velocity, chirp and phase, respectively. The auxiliary function  $\eta(x)$  is introduced for convenience and defines the type of the pulse. Specifically for a single soliton  $\eta(x) = 1$ , for two-soliton molecule  $\eta(x) = x$  and for three-soliton molecule  $\eta(x) = 4x^2 - 1$ .

It is instructive to start with considering the existence and dynamics of a single soliton on top of an inverted parabolic potential. The integration  $L = \int_{-\infty}^{\infty} \mathcal{L} dx$  using the trial function (34) with  $\eta(x) = 1$  gives rise to the following effective Lagrangian

$$\frac{L}{E} = \frac{1}{4}\tau^2\alpha_z - \xi_z^2 + \varphi_z + \frac{d_0}{\tau^2} + d_0\tau^2\alpha^2 + d_0\xi_z^2 - \frac{k_0}{4}\tau^2 - k_0\xi^2 - \frac{b_0E}{2\sqrt{\pi}\tau}. \quad (35)$$

where the pulse energy  $E = A^2\tau\sqrt{\pi/2}$  is conserved. Now applying the Euler - Lagrange equations with respect to the variational parameters, we get the ODE system for the pulse width and its center-of-mass position

$$\tau_{zz} = \frac{16d_0^2}{\tau^3} + 4d_0k_0\tau - \frac{4d_0b_0E}{\sqrt{\pi}\tau^2}, \quad (36)$$

$$\xi_{zz} = -k_0/(d_0 - 1)\xi. \quad (37)$$

The system for the two-soliton and three-soliton molecules will be similar, with only re-scaled energy coefficient,  $E \rightarrow E/4$  for the former case and  $E \rightarrow (41/320)E$  for the latter case (see the coefficient  $c_2$  in Eqs.(20)-(21)). As can be seen from this system, the center-of-mass and internal dynamics of the soliton are decoupled. This is due to the property of a parabolic potential and is the manifestation of the Ehrenfest's theorem (its validity for the nonlinear Schrödinger equation with a linear and parabolic potentials was proved in Ref. [22]). In other types of potentials these two degrees of freedom are coupled. In fact the equation for the center-of-mass is the harmonic oscillator equation with a purely imaginary frequency  $\omega^2 = k_0/(d_0 - 1) < 0$ , since in practical situations  $k_0 > 0$  and  $d_0 < 1$ . Therefore, the center-of-mass of the soliton is unstable against sliding down an inverted parabola with exponentially increasing distance from the origin

$$\xi(z) = \xi(0) e^{Kz}, \quad \text{where } K = \sqrt{k_0/|d_0 - 1|} > 0. \quad (38)$$

The equation for the pulse width (36) is similar to the equation of motion for a unit mass particle in the anharmonic potential

$$\tau_{zz} = -\frac{dU}{d\tau}, \quad U(\tau) = \frac{8d_0^2}{\tau^2} - 2d_0k_0\tau^2 - \frac{4d_0b_0E}{\sqrt{\pi}\tau}, \quad (39)$$

which is depicted in Fig. 4. The minimum of this potential is found from the solution of the quartic equation

$$\tau^4 - m\tau + n = 0, \quad m = \frac{b_0E}{\sqrt{\pi}k_0}, \quad n = \frac{4d_0}{k_0}, \quad (40)$$

and corresponds to the stationary width of the soliton. For a given pulse energy  $E$  this defines the shape of the soliton according to the ansatz (34). At some critical energy  $E_{cr}$  the local minimum in this potential disappears, which means

that Eq. (30) does not support solitons and molecules with energy below  $E_{cr}$ . The value of the critical energy can be found from the condition that Eq. (40) has a real solution, which takes place if  $m > 4(n/3)^{3/4}$ , or in terms of energy

$$E > E_{cr} = \frac{2^{7/2} \pi^{1/2}}{3^{3/4}} \cdot \frac{d_0^{3/4} k_0^{1/4}}{b_0} \simeq 8.8 \frac{d_0^{3/4} k_0^{1/4}}{b_0}. \quad (41)$$

In fact the shape of the potential  $U(\tau)$  gives the evidence that solitons and molecules in the system are meta-stable. In the same figure 4 we compare the pulse profiles obtained by solution of the stationary state Eq. (32) with the prediction of VA. The parameter  $\lambda$  for Eq. (32) is obtained using the shooting method, where the pulse energy  $E = \int |\varphi(x)|^2 dx$  is minimized and initial conditions  $\varphi(0) = A$ ,  $\varphi_x(0) = 0$  are used. As can be seen from this figure, the deviation between the two wave profiles is notable at far tails of the pulse, where the field intensity significantly decreases. The wavy tails on the numerically exact pulse profile, found from solution of Eq. (32) indicate the existence of waves reflected from (and partially transmitted through) the borders of the effective potential (31). The waves escaping the effective potential contribute to the continuous outflow of energy from the soliton propagating along the fiber, and that will be the fundamental source of its instability in conservative DM fibers.

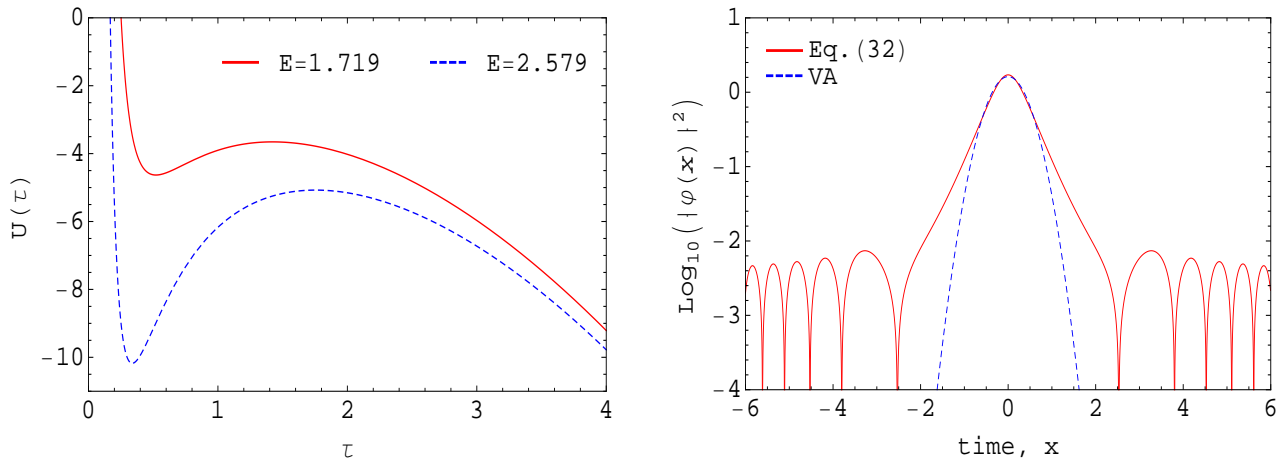


FIG. 4: Left panel: The potential (39) in the effective particle model of VA for two values of the pulse energy. The pulse with greater energy forms deeper potential well. The stationary amplitude and width of the soliton for  $E = 1.7193$ , according to VA are  $A = 1.6227$  and  $\tau = 0.521$  respectively. The existence of a local maximum and decay at large  $\tau$  is the evidence of meta-stability of the stationary state. Right panel: Comparison between the pulse shapes (in logarithmic scale) obtained by solving the stationary state problem (32) for  $\lambda = 4.6132$  and prediction of VA for the same pulse energy. The wavy tails are due to the interference of waves reflecting from the borders of the effective potential (31). Parameters  $d_0 = 0.3782$ ,  $b_0 = 3.0917$ ,  $k_0 = 0.6734$  are obtained using the VA Eqs. (16)-(17) for a single DM soliton with energy  $E_0 = 5.224$  (in original units  $\mathcal{E}_0 = 10$  pJ) and fiber data of Sec. II A.

The “pulse in the effective potential” picture, shown in Fig. 5, is helpful for the analysis of instability issues. The first aspect to be noted is that, the height and width of the effective potential barrier in both directions from the pulse are finite, and depends on the intensity of the pulse itself. Therefore a continuous and nonlinearly progressing energy outflow from the soliton takes place via the tunneling effect, whose rate can be estimated by means of the semiclassical WKB method as done for the matter-wave analogue of this problem in Ref. [28]. These authors also have shown that the rate of energy outflow (number of particles for condensates) nonlinearly increases, eventually leading to disintegration of the soliton. The second aspect is the instability of the center-of-mass position of the soliton against sliding down an inverted parabola. According to Eq. (38) any small departure of the center-of-mass position from the origin (the top of the inverted parabola) in either direction will exponentially grow.

To verify the above conclusions following from our model, we performed numerical simulations of the pulse propagation governed by Eq. (30). When we introduce the wave profile predicted by VA, which slightly differs from the solution of Eq. (32), as initial condition to Eq. (30), the pulse quickly adjusts itself by performing damped oscillations of its amplitude, and then continuously decay both in the energy and amplitude, as shown in Fig. 6. The frequency of oscillations of the amplitude well agrees with the prediction of VA, when we expand the potential (39) near its minimum  $\tau_0$  and estimate the corresponding frequency and period  $\omega_0 = \sqrt{d^2 U / d\tau^2}|_{\tau=\tau_0} \simeq 5.12$ ,  $T_0 = 2\pi/\omega_0 = 1.22$ . However, the VA does not take into account the dissipative effects. In numerical simulations we use the absorbing boundary technique [29] to prevent the interference of the soliton with the linear waves, otherwise reflected from the integration domain boundaries. To calculate the energy outflow from the soliton, we monitor the amount of energy



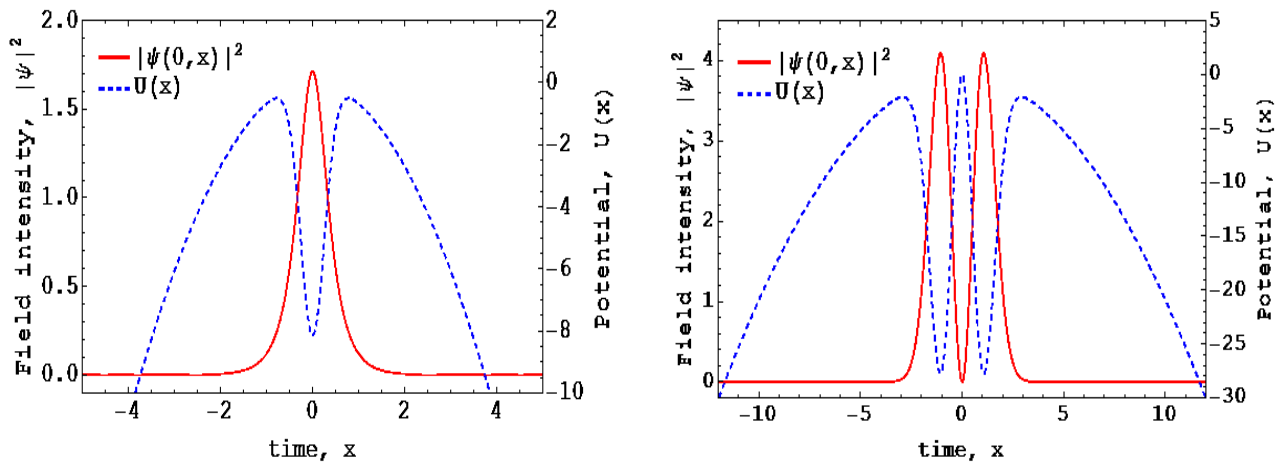


FIG. 5: Single soliton (left panel) and two-soliton molecule (right panel) of the averaged NLSE (30) are shown by red solid lines. The corresponding effective potentials according to Eq. (31) are shown by blue dashed lines. The parameters for the single soliton are the same as in previous figure, while for the two-soliton molecule the parameters are  $d_0 = 0.1978$ ,  $b_0 = 6.7274$ ,  $k_0 = 0.209$ ,  $E_0 = 10.448$  (in original units  $\mathcal{E}_0 = 20$  pJ).

in the central part of the domain ( $x \in [-2, 2]$  in Fig. 6) where the bulk of the pulse is confined. The energy loss rate  $dE/dz$  is characteristic for the fiber parameters and initial pulse power, which define the coefficients of the averaged NLSE (30). The instability of the center-of-mass position of the soliton is demonstrated in the middle panel of Fig. 6. If the calculation is performed with centering of the soliton, when at each step its center-of-mass is held at the origin, we observe complete disintegration of the pulse due to the energy loss, as shown in the right panel of this figure. The critical energy, at which the pulse disintegrates, according to the inset of the left panel is  $E_{cr} \simeq 1.2$ . This numerical finding is in good agreement with the prediction of VA Eq. (41)  $E_{cr} = 1.24$ .

In fact the above mentioned mechanism of energy loss sets the limit to attainable robustness of DM solitons and molecules in the given setup. The instability of the center-of-mass of the soliton will make it difficult to hold the pulse in the middle of its time slot. In Fig. 7 we demonstrate the propagation of two solitons governed by Eq. (30).

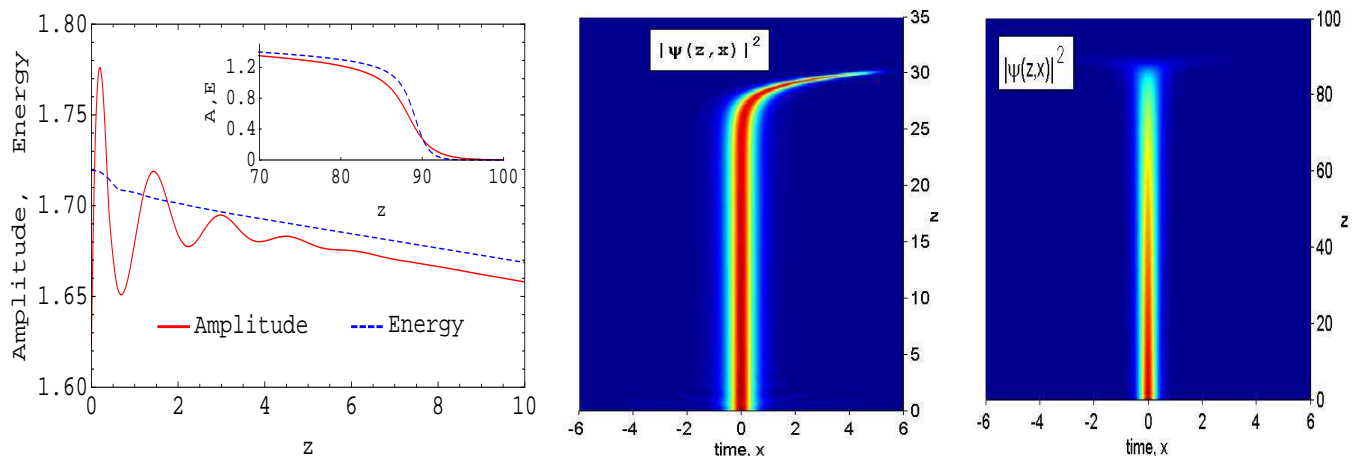


FIG. 6: Left panel: The amplitude and energy of the soliton decay as it propagates along the fiber due to the wave tunneling effect. The inset shows the nonlinear character of the energy loss at longer distances and abrupt disintegration of the pulse at some critical energy. The data is obtained by numerical simulation of Eq. (30) with absorbing boundary conditions. The initial wave is a Gaussian pulse with the amplitude  $A = 1.6227$  and width  $\tau = 0.521$ , as predicted by VA. Middle panel: The soliton slightly displaced from the top of the inverted parabola (by amount  $\Delta x \sim \pm 10^{-3}$ ) slides down with increasing velocity in the corresponding direction. This instability develops even due to a numerical noise, when the soliton is placed exactly at the origin  $x = 0$ . Right panel: When calculation is performed with centering of the pulse, a complete disintegration can be observed at sufficiently long propagation distance.

When two in-phase solitons are initially placed at a separation exceeding some critical value, they move apart with increasing velocity under the effect of the expulsive parabolic potential. If the solitons are placed at a smaller temporal

distance, they collide few times and merge together, and later the combined pulse develops instability, analogous to the single soliton case and slides down the inverted parabola. Similar behavior of two-soliton states were reported in the dissipative counterpart of Eq. (30) in Ref. [27]. An additional fact relevant to coupled soliton propagation in this system is that, the out-of-phase solitons always repel each-other and diverge from the origin in accelerated manner.

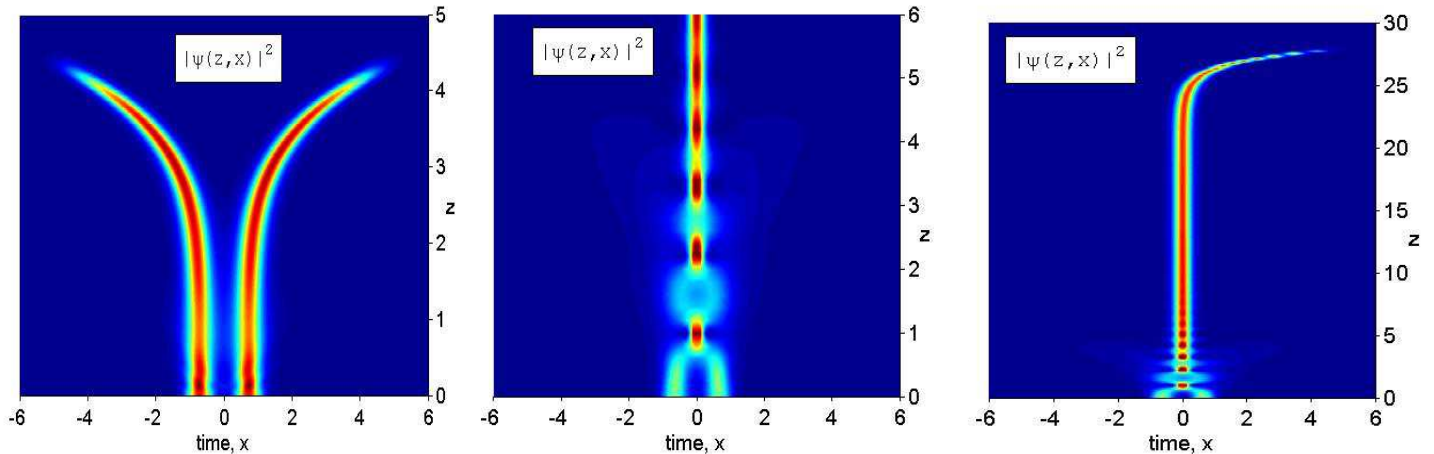


FIG. 7: Left panel: Two in-phase solitons placed sufficiently far from each-other ( $\Delta x = 0.72$ ) move apart. Middle panel: When solitons are placed at a distance ( $\Delta x = 0.65$ ) which is less than some critical value, they collide few times and merge. Right panel: Long distance behavior of the coalescent pulse (of the middle panel) is similar to the single soliton case, as its center-of-mass develops instability and slides down the inverted parabola.

The main result of our study of pulse propagation governed by the averaged NLSE (30) is that, it does not support truly stable solitons and molecules as the original DM Eq. (7) does. Rather it shows, that solitons and molecules in the conservative DM fiber are meta-stable, both in terms of energy and temporal position. In addition, the model of averaged NLSE allows to find the existence regimes and identify the limits of stability of solitons and molecules in DM fibers. The inclusion of dissipation and gain into the model may change the results to some degree. This will be a subject for separate study.

## V. CONCLUSIONS

We have developed a variational approximation which successfully describes the propagation of soliton molecules in DM fibers. The pulse shapes for a two-soliton molecule and three-soliton molecule, predicted by VA are shown to be sufficiently close to the numerically exact shapes found by solution of the original DM NLS equation. Then we have studied the dynamics of solitons and molecules in the averaged NLSE corresponding to the selected DM fiber system. The approach of averaged NLSE allows to identify the regimes of existence of solitons and molecules in the original DM system, and reveal the fundamental source of instability of soliton propagation in DM fibers, which is linked to continuous outflow of energy from the pulse due to the wave tunneling phenomenon. The model also predicts the instability of the temporal position of the pulse within its time slot. All calculations are performed using the parameters of the existing DM fiber setup [9, 10]. The model may provide guidance in further studies of the properties of soliton molecules in DM fibers.

## Acknowledgments

We thank F. Mitschke, A. Hause and E. N. Tsoy for valuable discussions. U.A.K. and B.B.B. are grateful to the Department of Physics of the KFUPM for the hospitality during their stay. This work is supported by the research grant UAEU-NRF 2011 and KFUPM research projects RG1214-1 and RG1214-2.

---

[1] Fedor Mitschke, *Fiber Optics. Physics and Technology* (Springer-Verlag, Berlin, Heidelberg, 2009).  
[2] M. Stratmann, T. Pagel, and F. Mitschke, Phys. Rev. Lett. **95**, 143902 (2005).

- [3] A. Hasegawa and F. Tappert, *Appl. Phys. Lett.* **23**, 142 (1973).
- [4] L. F. Mollenauer, R. H. Stolen, and J. P. Gordon, *Phys. Rev. Lett.* **45**, 1095 (1980).
- [5] A. Hasegawa and Y. Kodama, *Solitons in optical communications* (Clarendon Press, Oxford, 1995).
- [6] L. F. Mollenauer and J. P. Gordon, *Solitons in Optical Fibers: Fundamentals and Applications* (Academic Press, San Diego, 2006).
- [7] S. K. Turitsyn, G. B. Brandon Bale, and M. P. Fedoruk, *Phys. Rep.* **521** 135 (2012).
- [8] A. Hause, H. Hartwig, M. Böhm, and F. Mitschke, *Phys. Rev. A* **78**, 063817 (2008).
- [9] P. Rohrmann, A. Hause, and F. Mitschke, *Sci. Rep.* **2**, 866 (2012).
- [10] P. Rohrmann, A. Hause, and F. Mitschke, *Phys. Rev. A* **87**, 043834 (2013).
- [11] A. Maruta, T. Inoue, Y. Nonaka, and Y. Yoshika, *IEEE J. Selected Topics Quant. El.*, **8**, 640 (2002).
- [12] D. Anderson, *Phys. Rev. A* **27**, 3135 (1983).
- [13] S. K. Turitsyn, I. Gabitov, E. W. Laedke, V. K. Mezentsev, S. L. Musher, E. G. Shapiro, T. Schafer, and K. H. Spatschek, *Opt. Commun.* **151**, 117 (1998).
- [14] C. Pare and P. -A. Belanger, *Opt. Commun.* **168**, 103 (1999).
- [15] B. -F. Feng and B. A. Malomed, *Opt. Commun.* **229**, 173 (2004).
- [16] V. Cautauts, A. Maruta, and Y. Kodama, *Chaos* **10**, 515 (2000).
- [17] B. A. Malomed, *Soliton management in periodic systems* (Springer, 2006).
- [18] S. K. Turitsyn, *JETP Letters* **65** 845 (1997); S. K. Turitsyn, T. Schäfer, K. H. Spatschek, V. K. Mezentsev, *Opt. Commun.* **163**, 122 (1999).
- [19] J. H. B. Nijhof, W. Forysiak, and N. J. Doran, *IEEE J. Select. Topics Quant. El.*, **6**, 330 (2000).
- [20] Y. Kodama, S. Kumar, and A. Maruta, *Opt. Lett.* **22**, 1689 (1997).
- [21] K. H. Spatschek, S. K. Turitsyn and Y. S. Kivshar, *Phys. Lett. A* **204**, 269 (1995).
- [22] R. Hasse, *Phys. Rev. A* **25**, 583 (1982).
- [23] J. D. Moores, *Opt. Lett.*, **21**, 555 (1996).
- [24] K. Nakkeeran, *J. Phys. A: Math. Gen.* **34**, 5111 (2001).
- [25] C. C. Mak, K. W. Chow and K. Nakkeeran, *J. Phys. Soc. Japan* **74**, 1449 (2005).
- [26] Zhiyong Xu, Lu Li, Zhonghao Li, Guosheng Zhou, and K. Nakkeeran, *Phys. Rev. E* **68**, 046605 (2003).
- [27] R. Grimshaw, K. Nakkeeran, C. K. Poon, and K. W. Chow, *Phys. Scr.* **75**, 620 (2007).
- [28] L. D. Carr and Y. Castin, *Phys. Rev. A* **66**, 063602 (2002).
- [29] P. Berg, F. If, P. L. Christiansen, and O. Skovgaard, *Phys. Rev. A* **35**, 4167 (1987).